

Supplementary Information for

DYF-5/MAK-dependent phosphorylation promotes ciliary tubulin unloading.

Xuguang Jiang^{a,1}, Wenxin Shao^{a,1}, Yongping Chai^a, Jingying Huang^a, Mohamed A. A. Mohamed^b, Zeynep Ökten^b, Wei Li^c, Zhiwen Zhu^{a,2} and Guangshuo Ou^a.

^aTsinghua-Peking Center for Life Sciences, Beijing Frontier Research Center for Biological Structure, School of Life Sciences and Ministry of Education Key Laboratory for Protein Science, Tsinghua University, Beijing 100084, China;

^bCenter for Protein Assemblies, Physics Department, E22, Technical University of Munich, 85748 Garching, Germany; and

^cSchool of Life Sciences, Tsinghua University, Beijing 100084, China

¹X.J. and W.S. contributed equally to this work

²To whom correspondence may be addressed. Email: zhiwenzhu@126.com

This PDF file includes:

Figures S1 to S3
Table S1



Fig. S1. Amino acid mutations of in IFT-74 phospho-mimic (PM) and phospho-dead (PD) mutants.

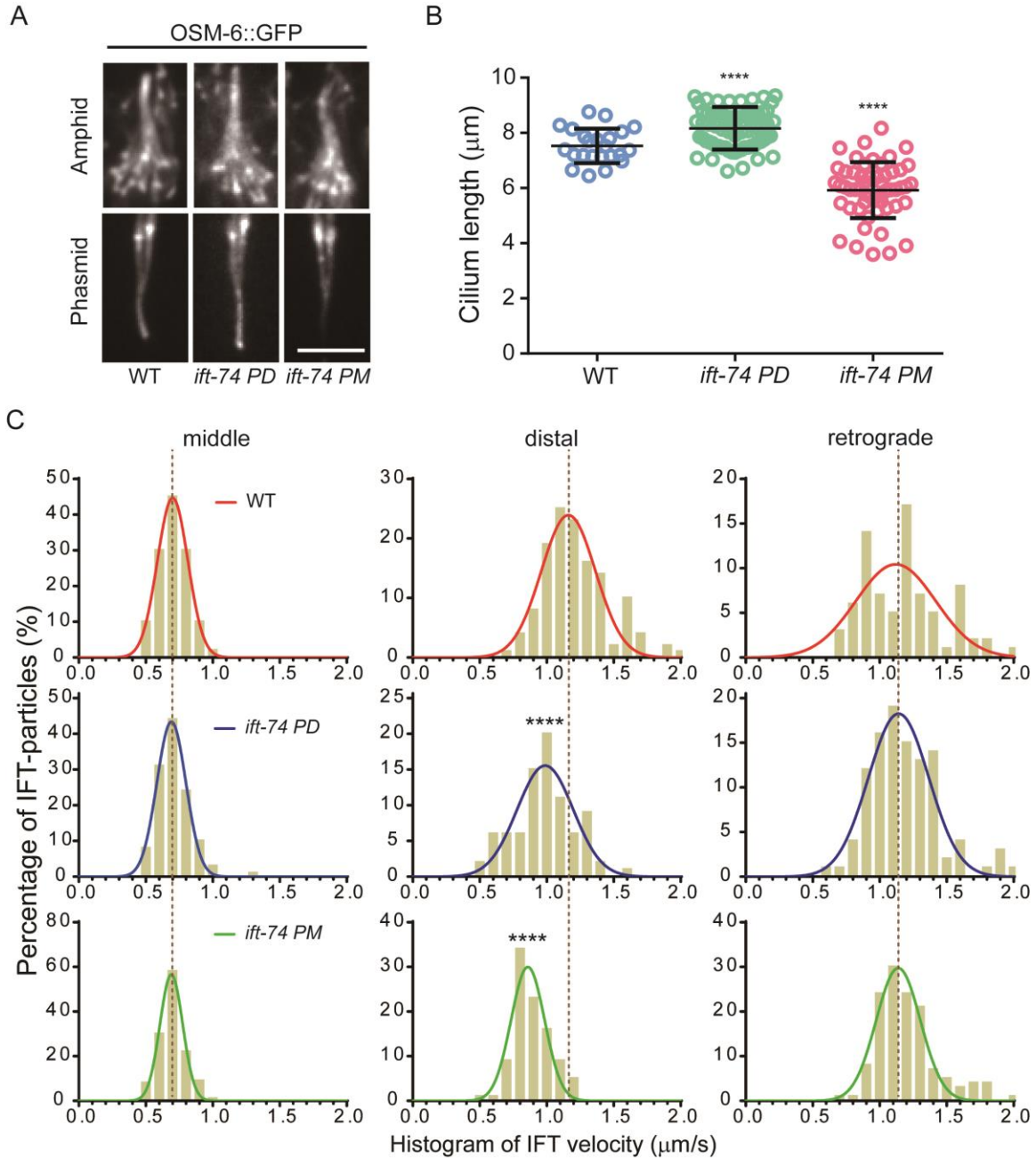


Fig. S2. Cilium morphology and IFT velocity in *ift-74 PM* and *PD* mutant animals based on *OSM6::GFP*. (A) Amphid (top) and phasmid (bottom) cilia morphology in *ift-74 PM* and *PD* mutants in comparison with wild-type (*N2*) animals. Cilia were imaged with GFP-tagged *OSM-6*. (B) Cilium length. Scale bar: 5 μm . (B) Cilium length in wild-type and *ift-74 PM/PD* animals (mean \pm SD; $n = 30$; **** $P < 0.0001$). *OSM-6::GFP* was used as the cilium marker. (C) Histogram of IFT velocities in wild-type and *ift-74*-mutant animals. Left: anterograde IFT along the middle segments. Middle: anterograde IFT along the distal segments. Right: retrograde IFT. *OSM-6::GFP* was used as the IFT marker for the measurement. Each plot was fit by a Gaussian distribution. Comparisons were performed between the wild-type and mutants. **** $P < 0.0001$.

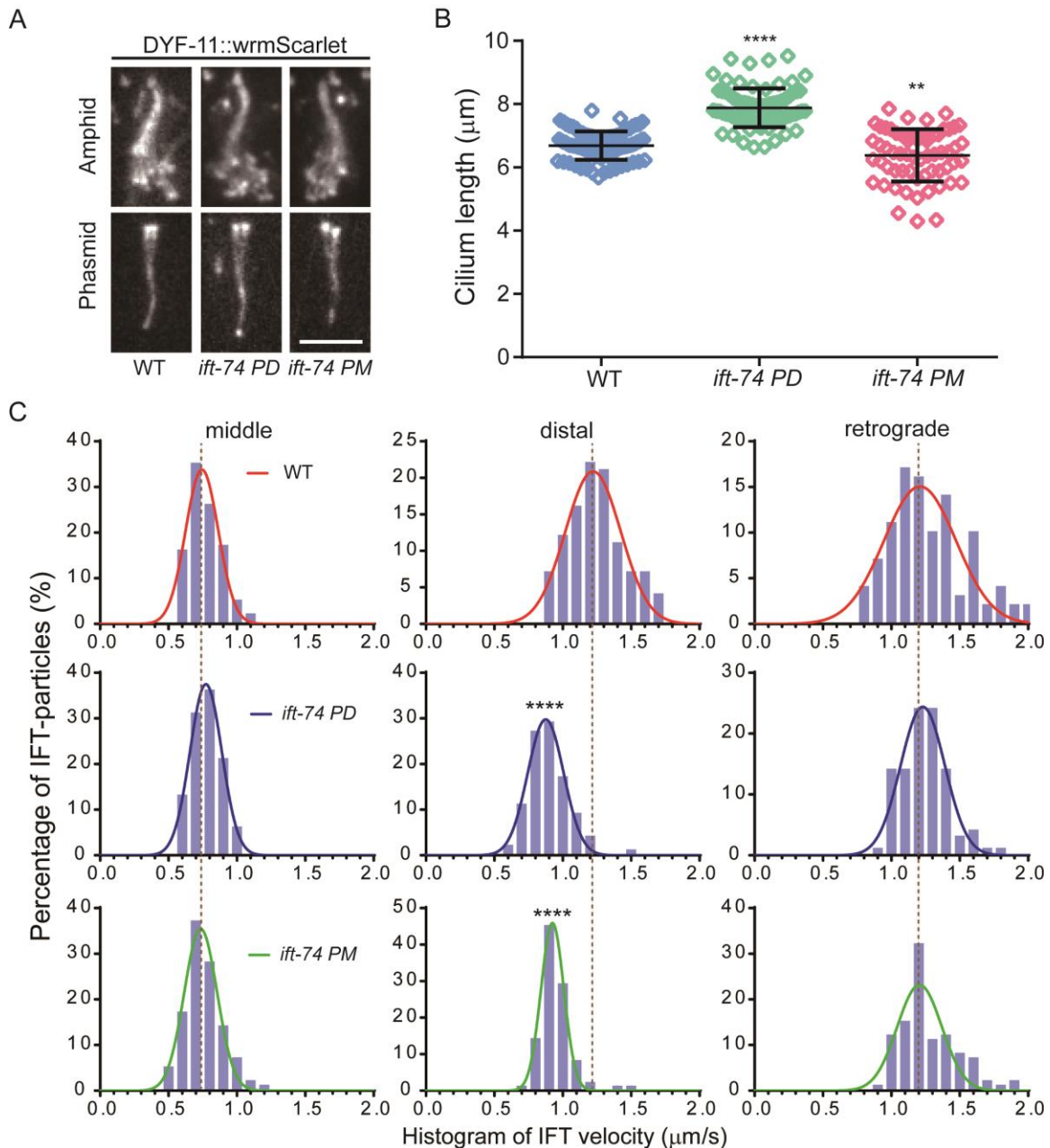


Fig. S3. Cilium morphology and IFT velocity in *ift-74 PM* and *PD* mutant animals based on DYF-11::wrmScarlet. (A) Amphid (top) and phasmid (bottom) cilia morphology in *ift-74 PM* and *PD* mutants in comparison with wild-type (N2). Cilia were imaged with wrmScarlet-tagged DYF-11. (B) Cilium length. Scale bar: 5 μm . (B) Cilium length in wild-type and *ift-74 PM/PD* animals (mean \pm SD; $n = 30$; $**P < 0.01$, $****P < 0.0001$). DYF-11::wrmScarlet was used as the cilium marker. (C) Histogram of IFT velocities in wild-type and *ift-74*-mutant animals. Left: anterograde IFT along the middle segments. Middle: anterograde IFT along the distal segments. Right: retrograde IFT. DYF-11::wrmScarlet was used as the IFT marker for the measurement. Each plot was fit by a Gaussian distribution. Comparisons were performed between the wild-type and mutants. $****P < 0.0001$.

Table S1. *C. elegans* strains used in this study

Strain name	Genotype	Method	Resource
N2	Wild type	/	CGC
GOU2362	<i>cas499 [ift-74::gfp knock-in]</i>	Microinjection	This study
SP1745	<i>dyf-5 (mn400)</i>	/	CGC
GOU4775	<i>dyf-5 (mn400); ift-74 (cas499)</i>	Genetic cross	This study
PHX4679	<i>syb4679 [ift-74 PD knock-in]</i>	Microinjection	Suny Biotech
PHX4674	<i>syb4674 [ift-74 PM knock-in]</i>	Microinjection	Suny Biotech
GOU4784	<i>ift-74 (syb4679); mnIs17 [osm-6::gfp unc-36(+)]</i>	Genetic cross	This study
GOU4785	<i>ift-74 (syb4674); mnIs17 [osm-6::gfp unc-36(+)]</i>	Genetic cross	This study
GOU4772	<i>cas1086 [dyf-11::wrmScarlet knock-in]</i>	Microinjection	This study
GOU4786	<i>ift-74 (syb4679); dyf-11 (cas1086)</i>	Genetic cross	This study
GOU4787	<i>ift-74 (syb4674); dyf-11 (cas1086)</i>	Genetic cross	This study
PHX4963	<i>syb4963 [ift-74 PD::gfp knock-in]</i>	Microinjection	Suny Biotech
PHX4964	<i>syb4964 [ift-74 PM::gfp knock-in]</i>	Microinjection	Suny Biotech